A SOLAR-POWERED WHITE LED-BASED UV-VIS SPECTROPHOTOMETRIC SYSTEM MANAGED BY PC FOR AIR POLLUTION DETECTION IN FARAWAY AND UNFRIENDLY LOCATIONS

P. Visconti [1], P. Primiceri [2], R. de Fazio [3] and A. Lay Ekuakille [4]

Department of Innovation Engineering, University of Salento, 73100, Lecce, Italy
Emails: paolo.visconti@unisalento.it [1], patrizio.primiceri@unisalento.it [2], roberto.defazio@studenti.unisalento.it [3], aime.lay.ekuakilly@unisalento.it [4].

Submitted: Dec. 2, 2016 ***Accepted: Jan. 17, 2017*** ***Published: Mar. 1, 2017***

Abstract – ***This research work regards the design and realization of an absorption spectrophotometer based on a LED light source in place of the usually employed Xenon lamp. The advantage of the use of LED technology resides in several factors such as the reducing of the analyte temperature variations and thus noise generation, which occur if a Xenon light source is used, beside of the high luminous efficiency, reliability, operating duration, lower maintenance and a lower power consumption. This last factor allows to supply the entire designed apparatus using a solar panel thus making the system easly portable for use even in places where the electricity network is absent. An optical filtering system was realized in order to detect the analyte absorption for each wavelength range selected by the optical filters. A PC-interfaced PIC-based control unit used to manage the different functionalities required by the spectophotometer was realized and tested. The control unit acquires and processes, via the developed firmware, the raw data provided by different sensors employed in the system. The sensors are used to monitor analyte temperature and humidity values, to control the analyte pressure and to acquire the luminous intensity value of the light beam before and after passing through the analyte. Finally, the realized electronic control unit actuates different mechanical sections (stepper motor, solenoid valve), sincronyzing and controlling the data exchange between hardware sections, microcontroller and the PC.***

Index Terms: Electronic control system, absorption spectroscopy, sensors, LED, PIC, firmware, measurements and prototype characterization.

I. INTRODUCTION

Aim of this paper is the design and realization of an electronic control system for spectrophotometric measurements using the LED-technology as radiation source [1-4]. This light source typology was chosen for its high luminous efficiency, reliability, operating duration, lower maintenance, low replacement costs and lower device cost compared to other radiation source beside the operating safety thanks to the lower operating voltage. Moreover, the white LED source, having lower driving voltage than Xenon arc lamp, usually used in spectrophotometer, allows to obtain a system with reduced power consumption. Furthermore, a LED light source due to the absence of IR component, allows to reduce the gas temperature variations due to radiation absortpion; this phenomenon occurs when a broad-spectrum light source (e.g a Xenon lamp) is used, resulting in noise generation [4, 5]. In particular, the *Lambert-Beer* law describes the electromagnetic radiation absorption phenomena that are the basis of the spectrophotometry: when a parallel radiation beam go through a solution layer with thickness l [m] and concentration c [mol/l] (figure 1), the incident radiation intensity I_0, due to interaction between photons and analyte absorbing particles, is attenuated resulting the transmitted light intensity equal to I_1. Thus, the gas *trasmittance* value is given by:

$$T = \frac{I_1}{I_0}$$

Moreover the gas *abosorbance* value is given by the following relationship:

$$A = -\log_{10} T = \log_{10} \frac{I_0}{I_1}$$

The *Lambert-Beer* law expresses the absorbance concept as following:

$$A = \varepsilon_\lambda * l * c$$

where ε_λ is the molar absorption coefficient or absorbivity expressed in m^2*mol^{-1}, that is a typical feature of each substance and strictly linked to the incident radiation wavelength.

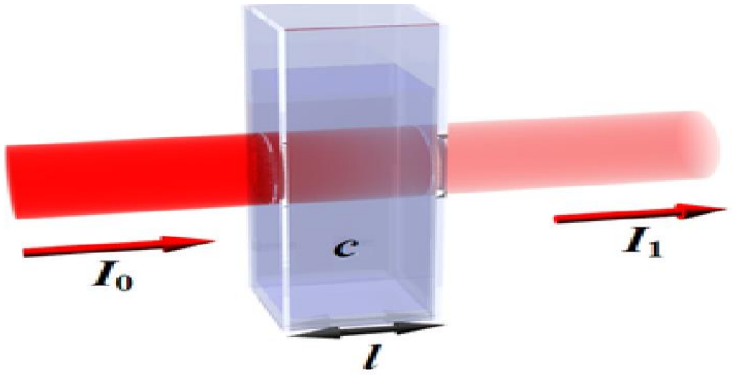

Figure 1. The interaction between photons and analyte absorbing particles reduces the light beam intensity of the incident radiation from I_0 to I_1.

The operation principle of absorption spectrophotometer is to identify and characterize the gaseous or lyquid analytes depending on their different interaction with used luminous radiation. There are several possible application fields of designed spectrophotometer, from gaseous/liquid pollutants detection up to indoor air quality monitoring in particular environments as surgery rooms [1-5].

In this work, the realized spectrophotometer can be powered by either the ac main voltage (to feed the 12V DC power supply) or with a solar panel (12V DC). This solution is possible thanks to the lower power consumption of the LED source, respect to other light source typologies, keeping low the power consumption of the whole system. In this way, the system power supply (12V) is provided by the battery charged by a solar panel [6, 7]. Therefore, the realized system results energetically autonomous and easily portable, so allowing to perform measurements even in places where the electrical power network isn't available, for example to detect air quality outside a laboratory, in a street or in a country-side.

The realized spectrophotometer employes an optical filtering system in order to test gas absorption in different UV/VIS wavelength ranges [4], [8]. A PIC-based electronic control unit manages the filtering system motion and controls the gas loading phases in the measurement chamber [9]. This last has a cylindrical shape with a plexiglass window on each base for light beam input/output and with three sensors installed inside for the acquisition of analyte temperature, humidity and pressure values [4], [10-15]. The used microcontroller interfaces with the different sensors [10, 11], acquires the raw data and processes them via firmware to obtain measured quantities. Furthermore, in order to evaluate the light intensity value passing through the analyte, the system includes a digital luminosity sensor interfaced with PIC. The aquired data from sensors are displayed on PC, through a microcontroller - PC serial communication, for an easy system monitoring during a complete measurement cycle.

II. SYSTEM FUNCTIONAL BLOCKS AND RELATED OPERATION

For the management of the spectrophotometer hardware section, the microcontroller PIC16F877A, which communicates with PC by serial interface, is used; it generates the square wave signal for filtering system driving, it controls the solenoid valve for managing gas flux into the chamber and it acquires data from the sensors present in the system. In figure 2, a broadly diagram of the spectrophotometer electronic section, with indication of the main functional blocks, is shown.

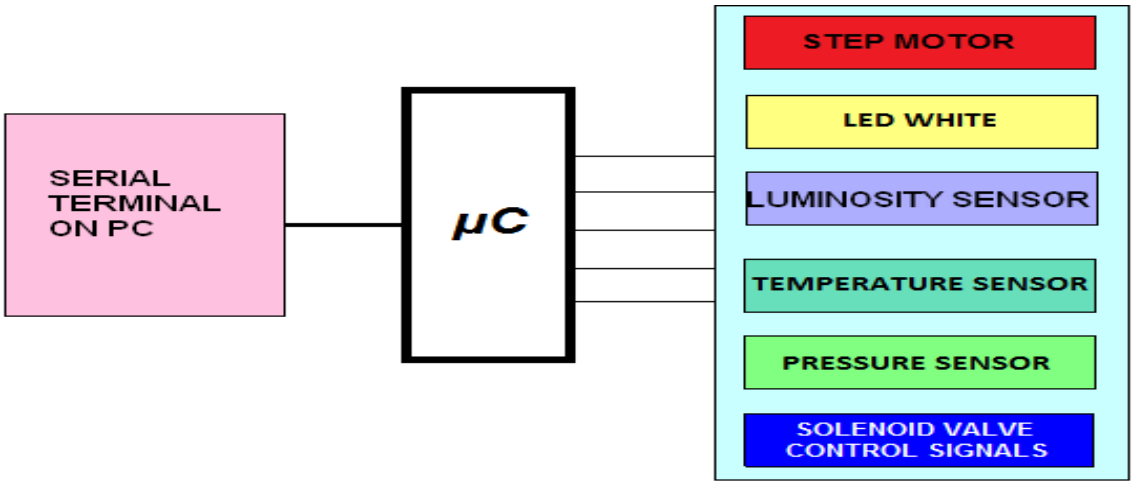

Figure 2. Main functional blocks of the spectrophotometer electronic section.

As shown in Figure 2, the main signals involved in the microcontroller-system communication, besides the serial communication with the PC, are the following:

- Signals microcontroller-temperature sensor.
- Signals microcontroller-pressure sensor.
- Signals microcontroller-luminosity sensor.
- Solenoid valve driving signals.
- Step motor driving signals.

In Figure 3, a detailed block diagram of the whole designed spectrophotometer is reported. The system is composed of the white LED source, a neutral optical filter holder used to reduce, if necessary, the light beam intensity, an optical filtering system consisting of six band-pass optical filters mounted on a filters wheel employed to select the desired wavelenght range, the measurement chamber containing the analyte, the different sensors, a solenoid valve and the microcontroller.

The working principle of the realized system is the following: the gas or liquid to be analyzed is loaded in the measurement chamber, placed along the radiation beam path downstream the filtering optical system, by means of the solenoid valve ("V" in figure 3) controlled from MCU. During this phase, the PIC acquires steadily pressure data provided from sensor located into the chamber. The luminosity sensor is placed in front of the chamber to detect light intensity level passing through the gas (transmitted radiation). This information allows to calculate gas absorbance value; also, varying the incident radiation wavelength range, by using optical filtering system and storing the transmitted luminous intensity values, the absorbance/ transmittance graph can be drawn as function of the selected wavelength range.

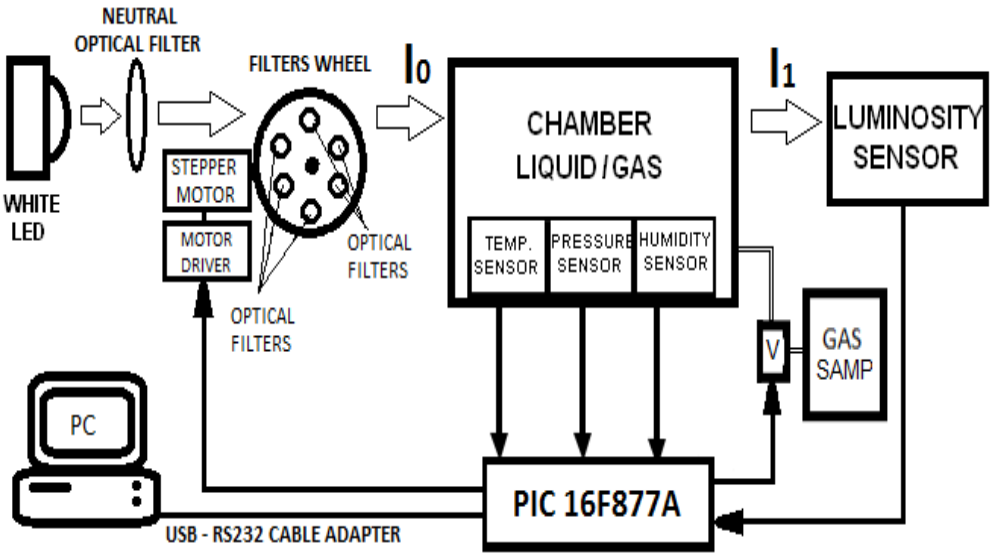

Figure 3. Block diagram of the designed spectrophotometer with indication of the main functional blocks (electronic, optical and hydraulic).

III. DESIGNED EXPERIMENTAL SPECTROPHOTOMETER: CIRCUITAL SCHEME AND EMPLOYED DEVICES

In figure 4, the circuital scheme of the designed spectrophotometer is shown. The MCU (PIC16F877A), which communicates via USART interface with the PC and manages the synchronization of the various components of the experimental apparatus, is the principal element. Another fundamental component is the radiation source, i.e. the white power LED described following, chosen for its large spectral range, between [380÷750nm], and for its high luminosity intensity. To perform the measures in different spectral intervals, the white LED source spectrum is divided in six different wavelenght ranges by the optical filtering system. It consists of a wheel, with mounted six different filters, actuated by a stepper motor driven by PIC. The designed system, shown in figure 4, includes two digital temperature sensors: the first one (model LM75A) is used to measure the instantaneous temperature inside the chamber; the second one (model DHT11) is only used to detect the analyte moisture, because of its long response time in the temperature measurement. Furthermore, in order to acquire the gas pressure into the measurement chamber, an analog pressure sensor (MPX6250) is used. For measuring the luminous intensity, the digital luminosity sensor (model TLS2561) is employed; it is located externally front of the chamber. Besides to managing and synchronizing of sensors and of the optical filtering system, the PIC drives the solenoid valve opening and closing, to allow the measurement chamber filling.

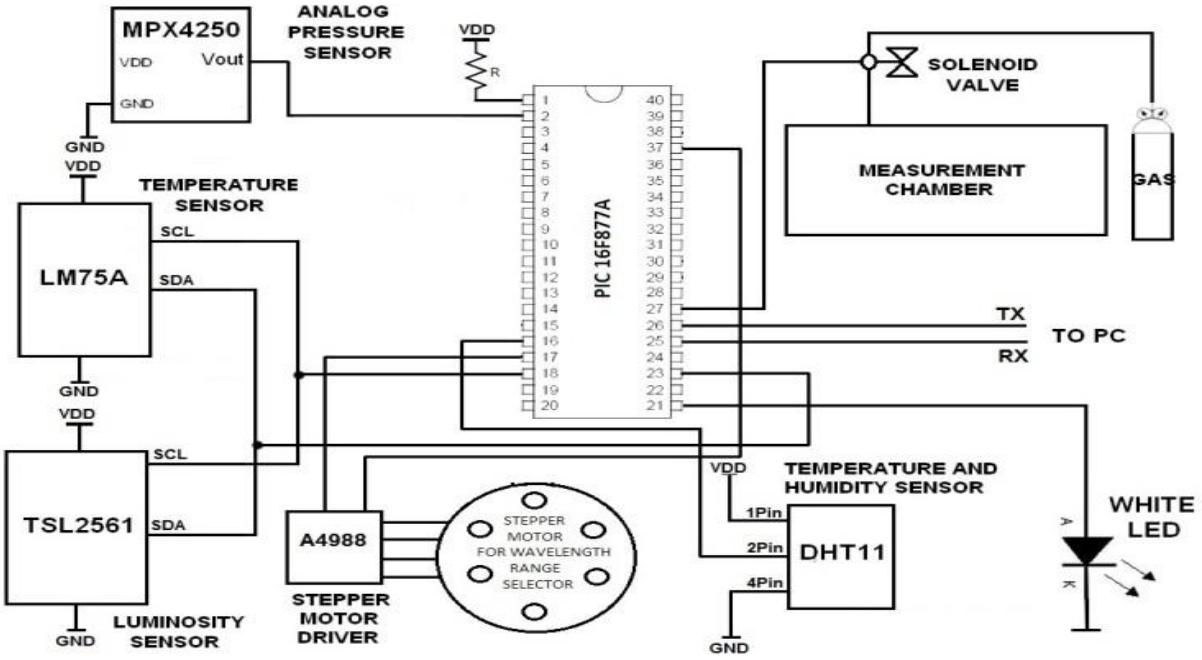

Figure 4. Circuital scheme of the designed spectrophotometer; the PIC16F877A manages the different sections highlighted in figure.

The system operation is the following: after an initial verification of chamber conditions (detecting temperature, pressure and humidity values), the revealed data are sent from MCU to PC and displayed on PC terminal. Subsequently, an illuminance measure for each optical filter is carried out with no gas in the chamber. In this phase, the acquired data are displayed on PC in order to be compared later with those acquired in presence of the analyte. Afterwards, MCU drives the opening of solenoid valve for loading the analyte in the chamber until its pressure is equal to the reference pressure value (previously set). At this point, once checked that chamber conditions respect set parameters, the illuminance measures are carried out, detecting also, in this case, gas pressure and temperature, for each optical filter. Therefore acquired data are shown on PC terminal allowing a real time monitoring by the user.

✓ *16F877A PIC FOR SENSORS DATA PROCESSING AND SYSTEM MANAGEMENT*

As aforementioned, the PIC manages and synchronizes the different tasks needed to achieve the desired behaviour of the entire system. The 16F877A PIC is a microcontroller, a microprocessor integrated on a single chip, that includes also non-volatile memory, RAM memory and peripherals that allow the communication with external devices, also named I/O peripherals. The main features are the following:

- 5V DC power supply (generally between 2V and 5.5 V);
- CMOS technology and TTL-compatible;

- low power consumption: <0.6mA @4MHz and 1µA @stand-by;
- high output current 25mA sink/source;
- 4-wire JTAG interface for programming;
- clock frequency up to 20MHz;
- 33 independent I/O digital lines, organized in 5 ports;
- 10bit A/D converter and 8 analog input multiplexed;
- 1 USART port and 1 standard synchronous serial port SPI and I^2C;
- two PWM modules for power control.

The used microcontroller is provided of several configuration registers (i.e. for addressing, state, storing, configuration and control) but also of one ALU (Arithmetic Logic Unit) to perform arithmetic and logic operation. It also includes other several circuital blocks to be used as function of the specific application. The use of the PIC, in this research work, is essential in order to acquire data detected by sensors; in particular, the MPX6250 analog pressure sensor is intefaced with PIC using the integrated Analog-Digital Converter module, whereas the communication with the DHT11 temperature-humidity digital sensor occurs by *one-wire*® communication interface, as described following. The TSL2561 luminosity and LM75A temperature sensors are both interfaced using the I^2C communication protocol; it's a serial standard that allows to link, on the same bus, several devices with just two wires (one for clock and the other for detected data), where each device is called up by using the proper device address. Another advantage of the I^2C protocol is the possibily to add or remove device without changing the circuital configuration. The two dedicated lines are SDA (Serial Data) and SCL (Serial Clock); the first one is dedicated to the data transit in byte format, whereas the second one is used for clock transmitting needed to transmission synchronization.

✓ *POWER WHITE LED SOURCE AND NEUTRAL FILTERS*

The utilized light radiation source is shown in figure 5a; it integrates a white power LED, model *XLamp XM-L T6* produced by CREE (figure 5b), which presents a small size and high output luminous flux (> 1000 lm, with a light beam collimated by a proper lenses system); its emission spectrum is reported in figure 5c (in blue color). Furthermore, a luminous power density equal to 205mW/cm^2 (referred to area of ~1.7cm^2) was measured. The *XM-L T6* Cree LED presents a typical forward voltage equal to 3.1V corrisponding to a forward nominal current of 1500mA; its maximum driving current is equal to 3000mA at which it provides an

output light of 1040 lm. In order to regulate the beam intensity, depending on the different analyzed gas typology, neutral filters, shown in figure 6, (model Thorlabs ND01B or ND03B or ND05B as function of the desired attenuation) can be used; they allow to reduce the intensity of radiation rispectively by 79% (ND01B), 50% (ND03B) and 32% (ND05B). The optical neutral filters can be placed in front of the LED radiation source, as shown in figure 3.

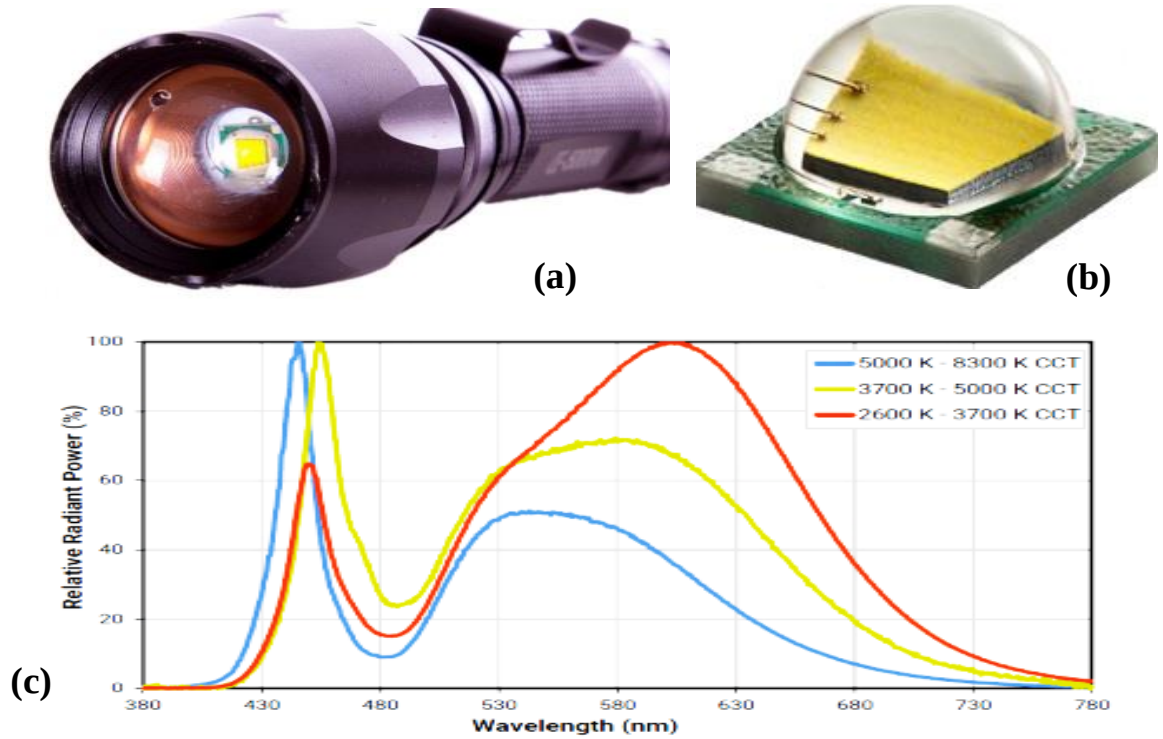

Figure 5. Flash-light that incudes the white LED *XLamp XM-L T6* and the optical lenses (a), view of the white LED *XLamp XM-L T6* (b) and its emission spectrum with the color temperature as paramenter (5000K is used in this work) (c).

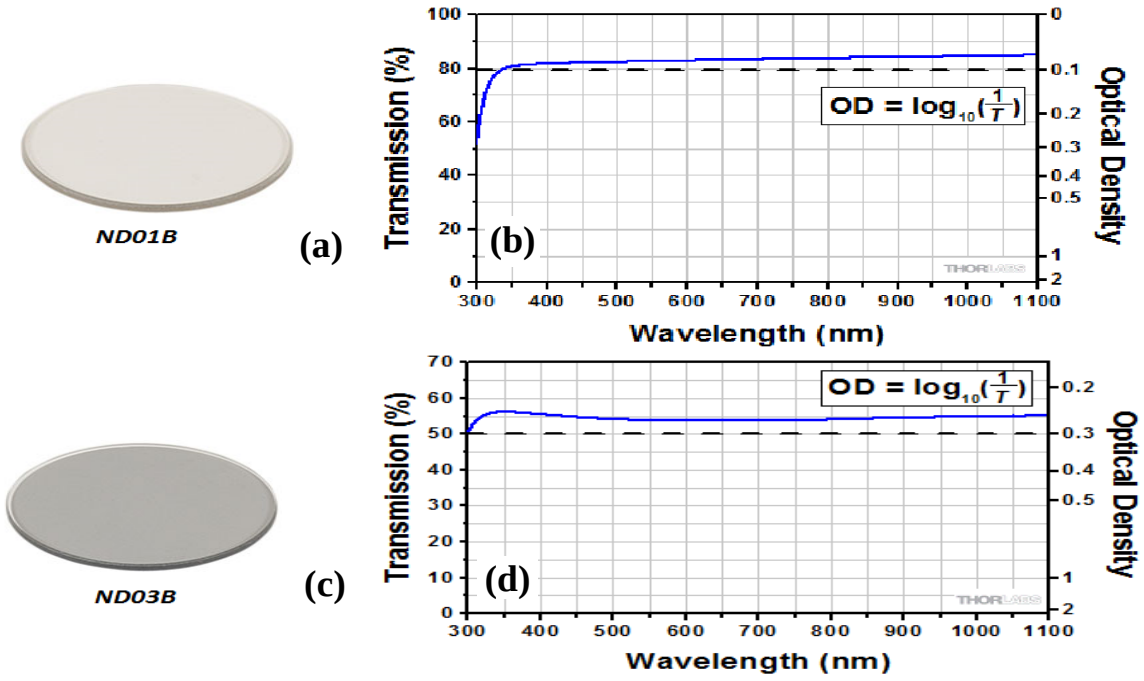

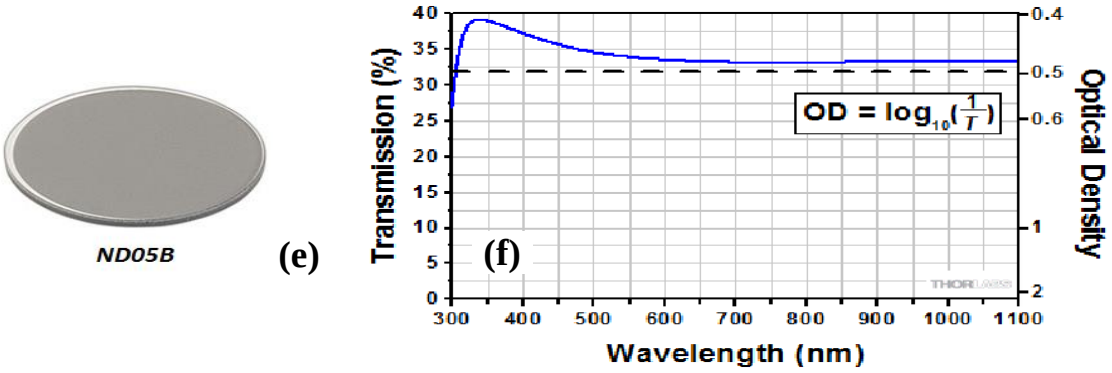

Figure 6. Neutral filters used to vary the radiation beam intensity as function of their transmission spectrum: Thorlabs model ND01B (a)-(b), ND03B (c)-(d) and ND05B (e)-(f).

✓ *USED LUMINOSITY, PRESSURE, TEMPERATURE, HUMIDITY SENSORS AND THEIR TECHNICAL FEATURES*

To detect transmitted light intensity for each wavelength range, the *Light to digital Converter TSL2561* produced by TAOS, shown in figure 7a, is used, whereas in the figures 7b and 7c, the TSL2561 luminosity sensor with package version FN embedded on a proper small board to semplify the circuital connections is shown. The sensor detects infrared and visible radiation using two photodiodes, providing a response like that of the human eye (figure 8a). It converts the two photocurrents in digital format using two integrated analog to digital converters (figure 8b) and it stores the data in two 16 bit buffer registers, *Channel0* and *Channel1*. Therefore, it's a digital sensor with 16bit resolution able to detect light intensity between 0.1 and 40kLux; its spectral response covers the interest wavelenght range [380÷750]nm as shown in figure 8a. The digital output signal is available using I^2C protocol; the microcontroller (master) sends a proper command sequence to read the stored value in the sensor buffer registers. Once received the raw data, the MCU extracts illuminance values using a suitable conversion function implemented in the installed firmware.

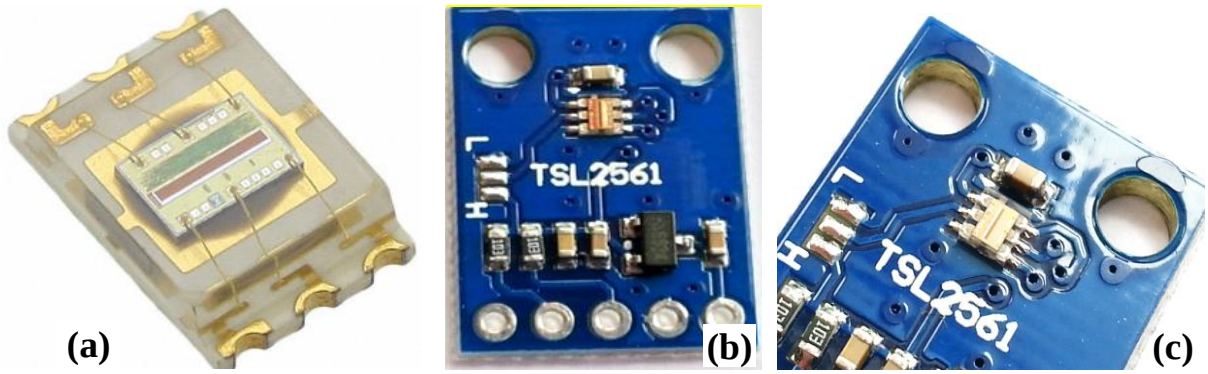

Figure 7. Luminosity sensor *TSL2561* FN package (a), same sensor mounted on a small board to facilitate its connection with the MCU (b) and its magnification (c).

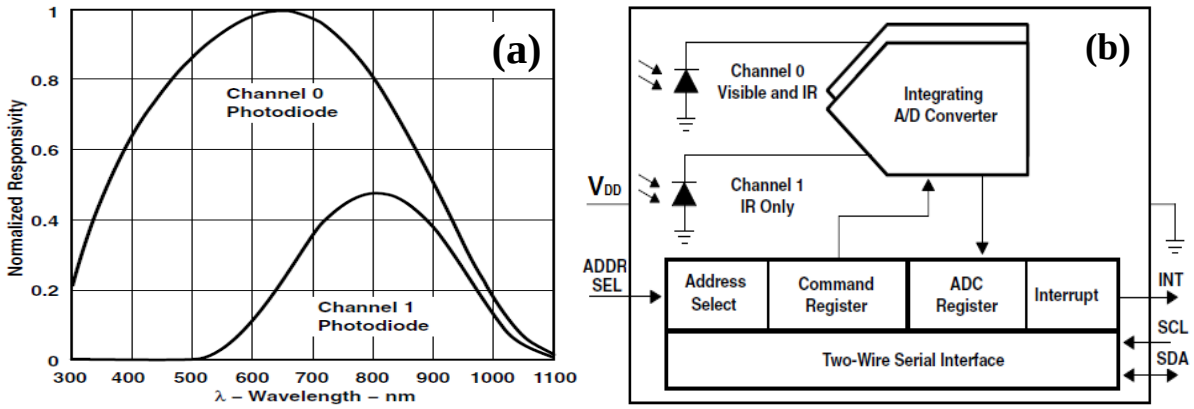

Figure 8. Spectral responsivity of the two photodiodes integrated in the TSL2561 sensor (a) and simplified internal block diagram of the TSL2561 light sensor (b).

The figure 9 shows the reading protocol from luminosity sensor TSL2561. The expected command sequences are: for starting communication, the master (MCU) sends a start sequence, followed by slave address with write indication (01110010) and waits for the slave acknowledgement. Once received the ack, the master sends the command indication including the buffer register address (10001100). Next, after a start repeat sequence, MCU sends again the slave address, but with the read indication (01110011). After the acknolodgement reception, the MCU can read the bytes contained in the buffer register. Subsequently, MCU (master) sends a acknolodgement signal and then it can send a stop sequence.

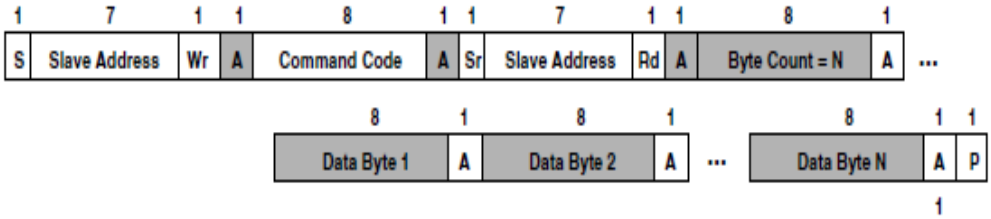

Figure 9. Command sequences related to I^2C protocol for communication between MCU and TLS2561 digital sensor to acquire the luminosity data downstream the measurement chmber.

In order to detect the gas pressure value, an analog pressure sensor, model *MPX6250* produced by *NPX Semiconductors*, shown in figure 10a, is used. It is a piezoresistive pressure sensor realized in monolithic silicon designed for microcontroller applications. The sensor allows to measure pressure values in the range [0 ÷ 250] KPa, with a response time equal to 1ms and with accuracy of $\pm 1.4\%V_{FSS}$. The typical circuital configuration is shown in the figure 10b; in this work, the output signal is acquired by PIC's A/D conversion module. The figure 10c shows the block diagram of internal circutry integrated on pressure sensor chip. The pressure detected by the sensor is acquired by the microcontroller and processed via firmware to extract the chamber pressure value, operation very simple since the sensor presents a linear transfer function as shown in the figure 10d.

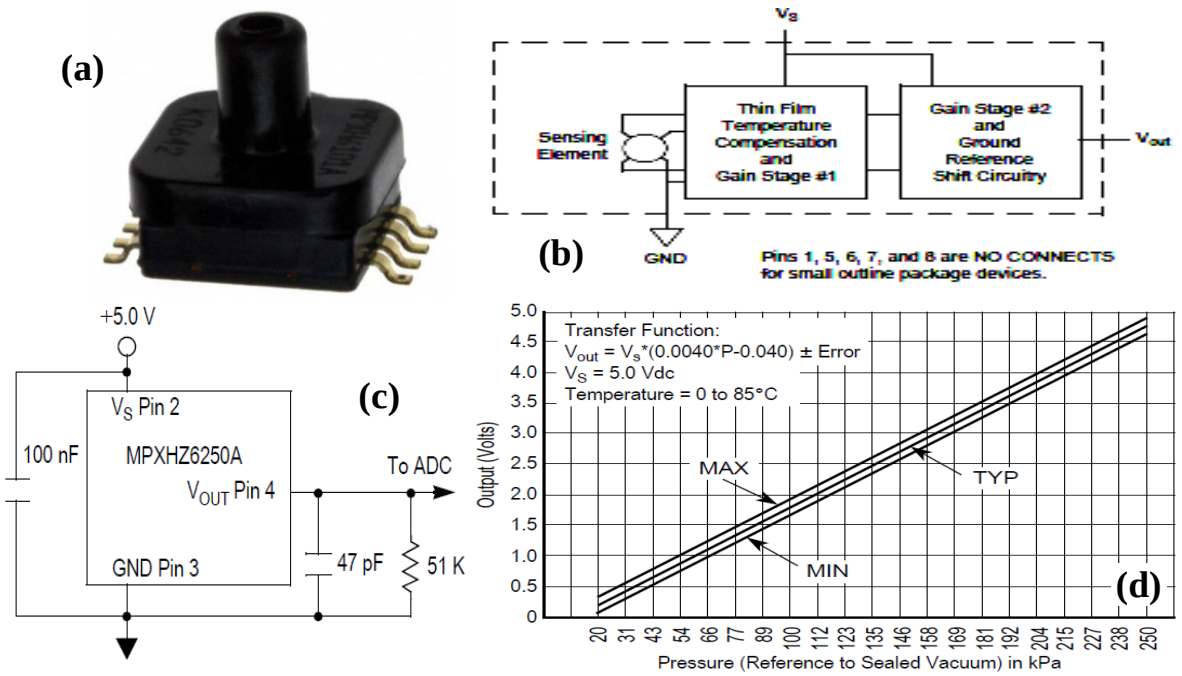

Figure 10. View of *MPX6250* analog pressure sensor (a), MPX6250 internal scheme (b), typical application circuit (c) and its transfer function: Output Voltage vs Pressure [kPa] (d).

LM75A digital temperature sensor (figure 11a) is used to measure the gas temperature within the chamber. It's a temperature to digital converter with a resolution of 0.125°C and it is provided of an ΣΔ A/D converter (figure 11b) with 11-bit resolution. The temperature digital data are stored in a buffer register (*Temp*) with an 11-bit 2'complement format. The sensor operates in *normal mode* as defined in the datasheet, i.e. the reading is performed and updated in the *Temp* register every 100ms. To read detected temperature value, the MCU sends proper command sequence to the sensor using I^2C comunication protocol, as expected by datasheet.

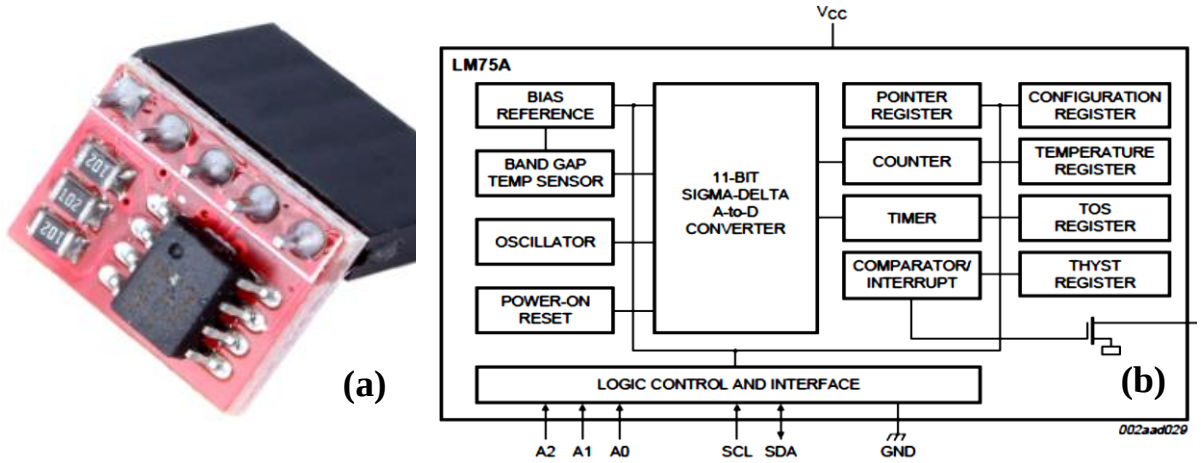

Figure 11. View of the *LM75A* temperature sensor placed on its specific small PCB (a) and its simplified internal block diagram (b).

The moisture measure within the measurement chamber is performed by the *DHT11* temperature-humidity sensor shown in figure 12a. The sensor can acquire humidity values in

the range [20 ÷ 90]% with a 1% resolution. The output digital signal is provided by using the one-wire comunication protocol. Figure 12b shows the typical circuital configuration used to acquire the detected temperature and humidity data from the microcontroller (µC).

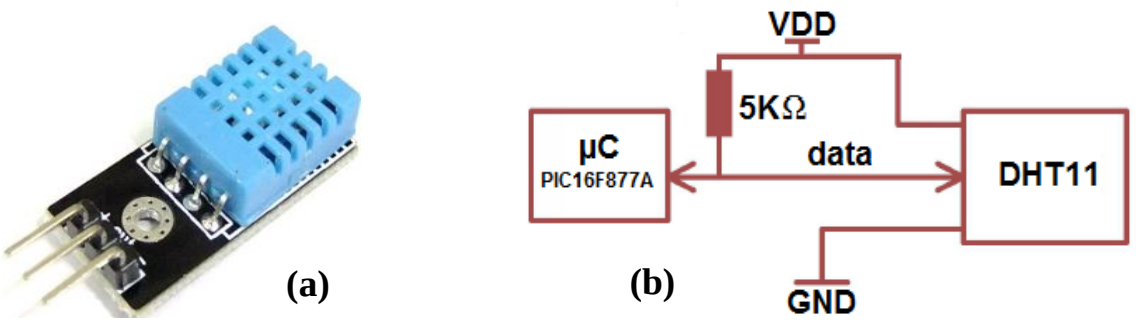

Figure 12. Front view of *DHT11* Temperature and Humidity sensor (a) and circuital scheme used to connect the µC, employing the 5kΩ pull-up resistor, with the DHT11 sensor (b).

The moisture reading process is articulated as follow: once the MCU sends the reading request, the sensor responds sending the data packet, as reported in figure 13. Data packet consist of 40 bits, divided in the following way:

***Data** = 8bit humidity integer data + 8bit humidity decimal data + 8bit temperature integer data + 8bit fractional temperature data + 8bit parity bit*

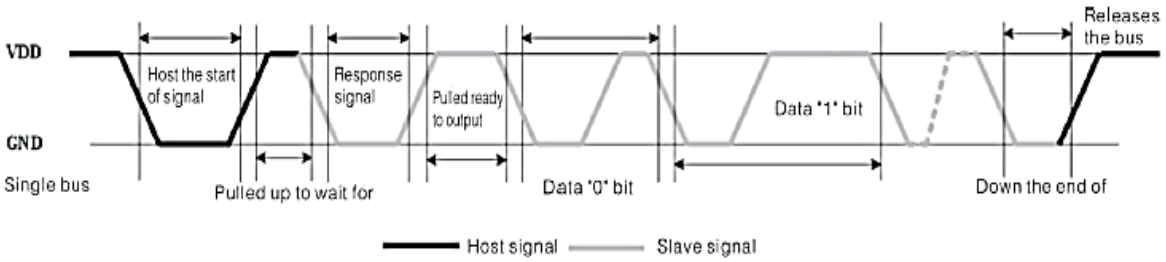

Figure 13. Data timing diagram of the acquisition by MCU from the DHT11 sensor used to detect the gas humidity in the chamber.

The time duration of the whole communication cycle is 4ms. The information relative to the logical value of each bit isn't contained in the signal level, but it depends on the signal duration; for the logical value "0" the provided signal is 0V for 50µs passing to 5V for 26÷28 µs, whereas for the logical value "1", the signal is newly low for 50µs rising to 5V and maintaining this value for 50÷70µs, as reported in figure 14.

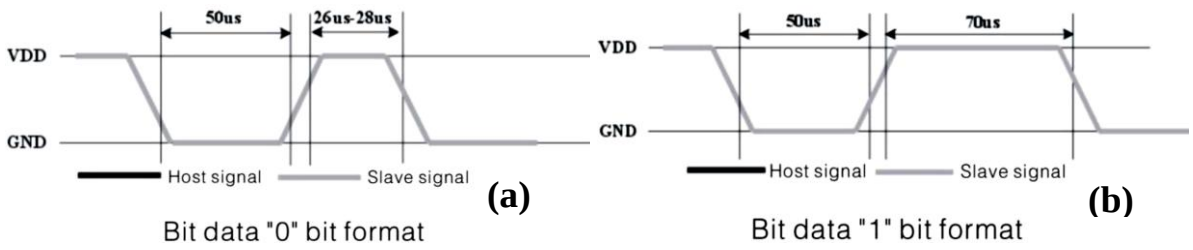

Figure 14. Signal shape related to the logical value "0" (a) and to the logical value "1" (b) provided by the DHT11 sensor.

✓ *A4988 STEPPER MOTOR DRIVER FOR LIGHT WAVELENGTH SELECTION AND USED SOLENOID VALVE*

The filtering system, realized to select the desired wavelenght range by means of the mounted optical filters, consists of a filters wheel rotated by a stepper motor. This last is driven by the bipolar stepper motor driver A4988 shown in figure 15a. It's featured by adjustable current limit, over current and over temperature protections, by 5 different step resolutions (down to 1/16 step); it operates from 8V to 35V and it can deliver up 1A per phase. The circuital scheme of the PCB, on which the A4988 stepper motor driver is mounted, is reported in figure 15b, whereas, the figure 15c shows a typical circutal configuration with the A4988 driver connected to a microcontroller for driving of a 2 phases stepper motor.

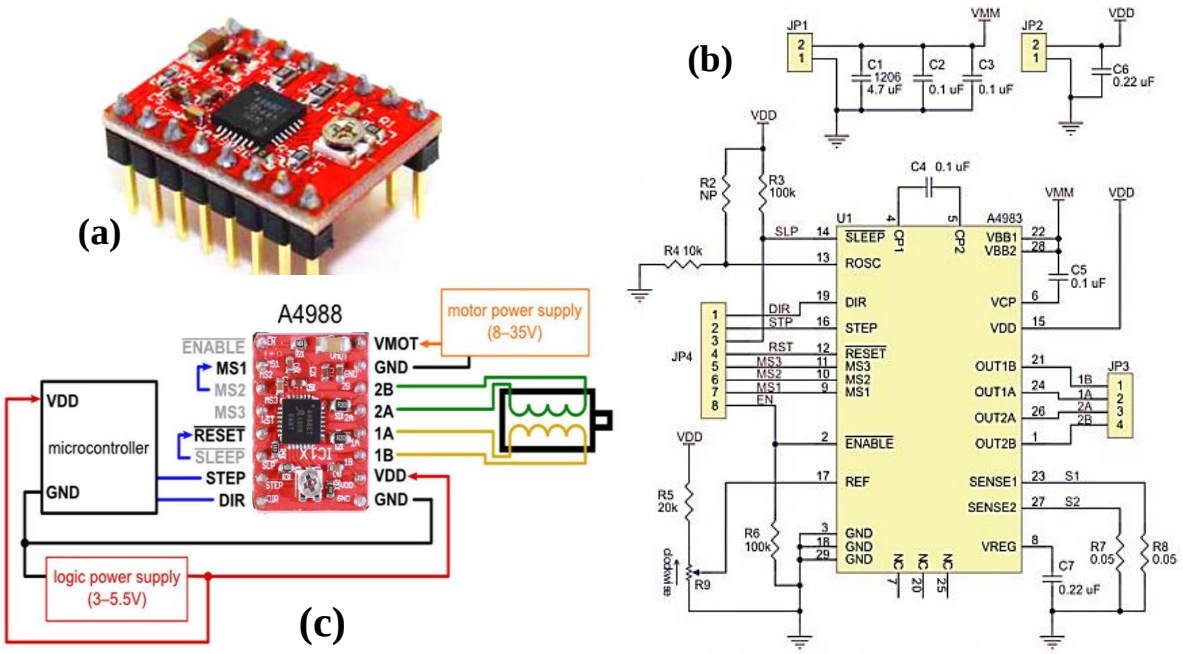

Figure 15. A4988 stepper motor driver on its small PCB (a), circuital scheme of the stepper motor driver board (b) and view of connections between A4988, MCU and stepper motor (c).

In order to handle the chamber filling and emptying with the analyte, the system is provided of the solenoid valve model 6011 produced by *Burkert* (shown in figure 16).

Figure 16. Burkert 6011 solenoid valve used to handle the chamber filling and emptying.

It's a compact device suitable for all the applications that involve the managing of gas or liquid. Its main features are the following: pressure range equal to 0÷6 bar, 12V DC power supply and operating temperature between -10 ÷ 100°C. For driving of the solenoid valve, the use of a DC-DC step-up converter is needed because the voltage and current values, 5V and 25mA, provided by one microcontroller's pin are not suitable. In fact, considering the valve power consumption of 4W and the 12V DC driving voltage, as reported in the datasheet, the valve operating current is given by:

$$P = V * I \rightarrow I = \frac{P}{V} = \frac{4W}{12V} = 333mA$$

Therefore, the DC-DC step-up converter, described in detal following in paragraph V, has to be able to provide 12V and more than 333mA as output current.

IV. OPTICAL FILTERING SYSTEM, STEPPER MOTOR FOR FILTER WHEEL DRIVING AND LIGHT COLLIMATION SETUP

The filtering system, shown in figures 17 (a and b), is used to select different wavelength range of emission spectrum [380÷750]nm of white-LED radiation source, as reported in [4].

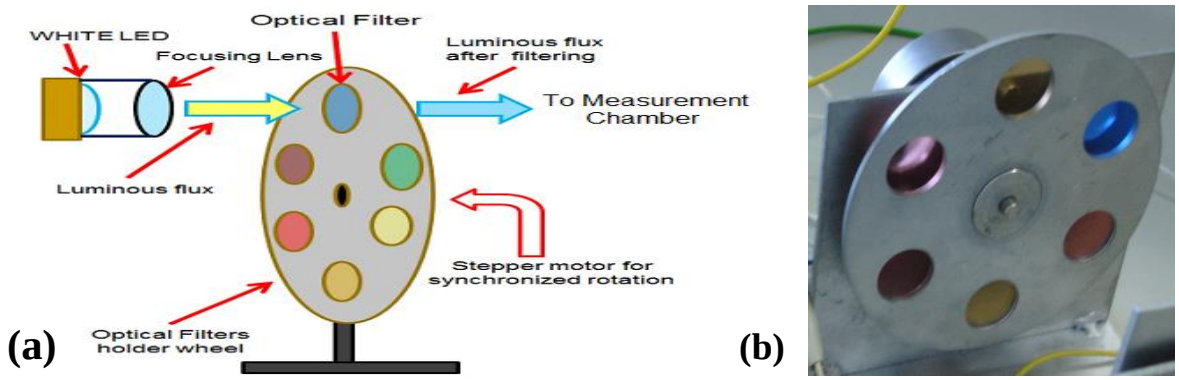

Figure 17. Basic operating principle of the optical filtering system (a) and view of the realized system actuated by a stepper motor (Nema 17) (b).

The Nema 17 (shown in figure 18) is a stepper motor with dimension (43.2 x 43.2)mm, usually used for 3D printer and other equipments such as CNT machines; its main features are the following:

- 2 phases;
- from 1.5A to 1.8A current per phase;
- square wave as driving voltage (4V for high voltage value);
- 3 to 8 mH inductance per phase;
- 44 N*cm or more as holding torque;
- 1.8 or 0.9 degrees for each step.

Figure 18. Nema 17 stepper motor used to actuate the optical filtering system.

The PIC manages accurately the wheel progress so that the optical filters sequentially pass in front the white LED, thus selecting the different wavelength ranges. The chosen optical filters, produced by Thorlabs and Andover, divide the LED source spectrum in six equal parts. The used models are FGB25 [315-445]nm (Thorlabs), FGB7 [435-500]nm (Thorlabs), FGV9 [485-565]nm (Thorlabs), 600FS80 [560-640]nm (Andover), FB650-40 [630-670]nm (Thorlabs) and 700FS80 [660-740]nm (Andover). Each of them is an optical bandpass filter with diameter 25mm and thick 2mm in order to fully cover the hole of the filter holder wheel. Their transmission spectrum allows to uninterruptedly cover the source spectrum. The figure 19 shows the real photos of the chosen filters and the relative transmission spectrum.

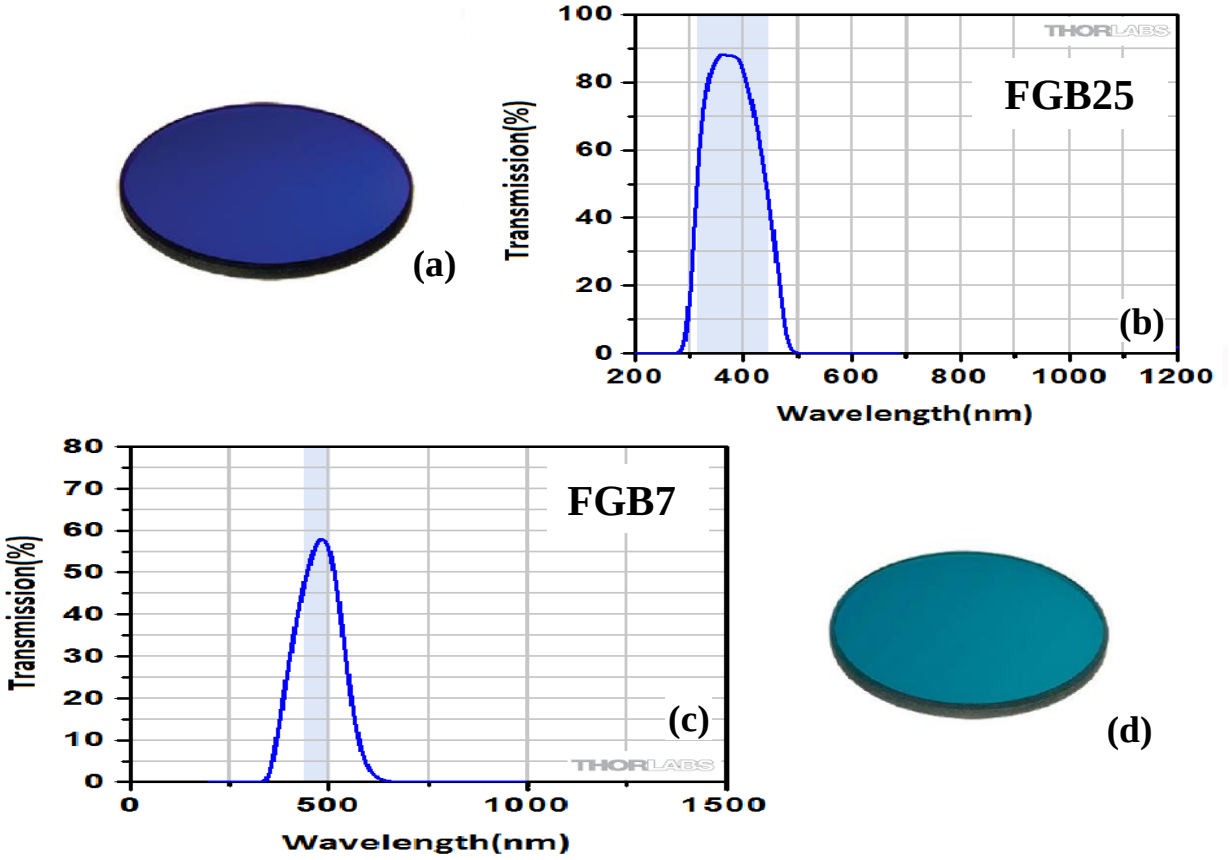

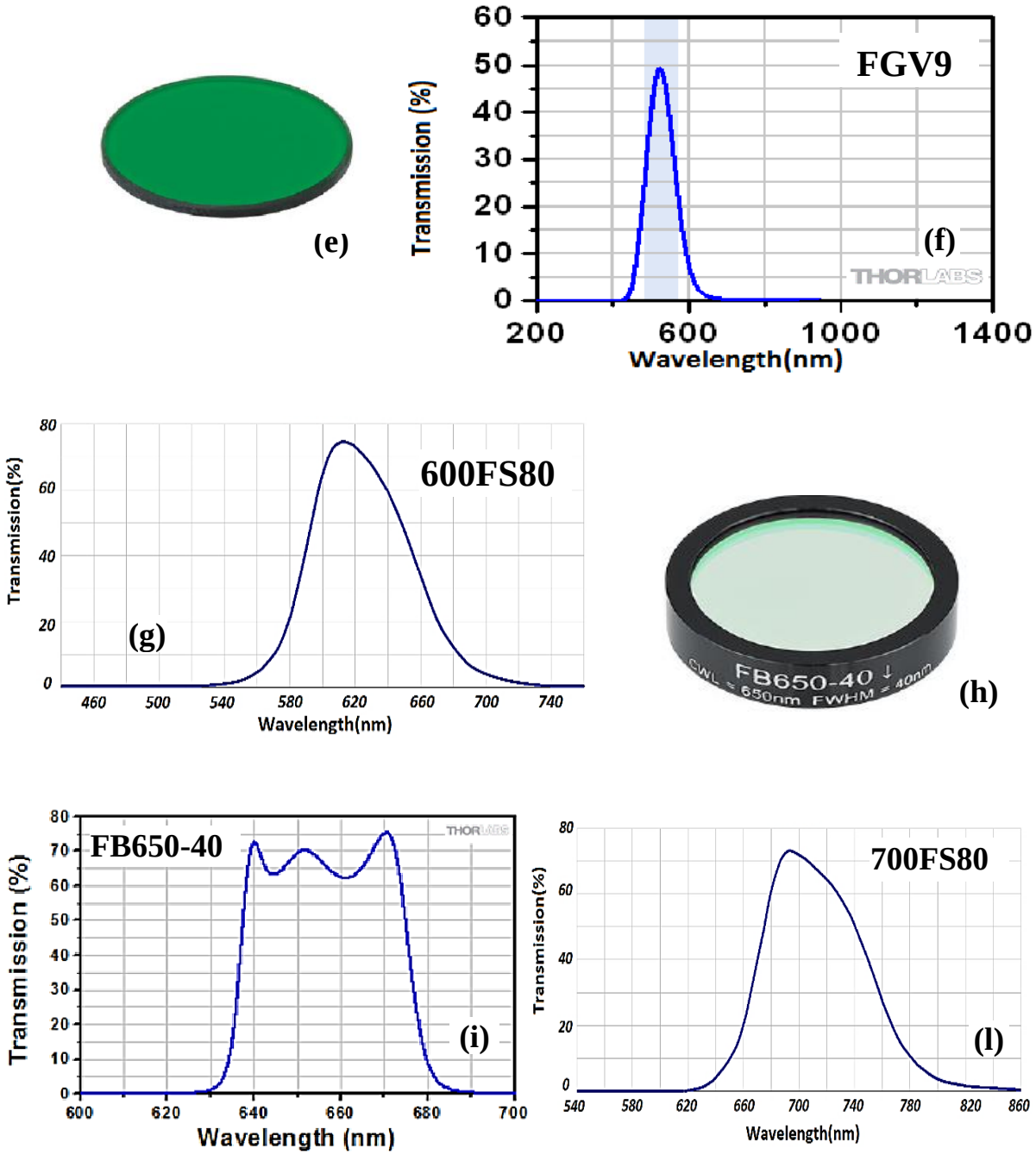

Figure 19. Bandpass optical filters chosen to divide the LED source spectrum in six intervals. FGB25 model (a) and its transmission spectrum (b), filter FGB7 (d) with transmission spectrum (c), filter FGV9 (e) and its transmission spectrum (f), transmission spectrum of the filter model 600FS80 (g), FB650-40 (h) with transmission spectrum (i) and finally 700FS80 transmission spectrum (l).

To collimate the radiation beam and to reduce its size, the cascade of two lenses is employed, one with focal length double than the other; they are placed just front of the LED radiation source (as reported in figure 20). The chosen lenses are: *LA1050* (focal length equal to 10cm) and *LA1979* (focal length = 20cm). They are positioned to a distance, between them, equal to the sum of the two focal lengths (30cm).

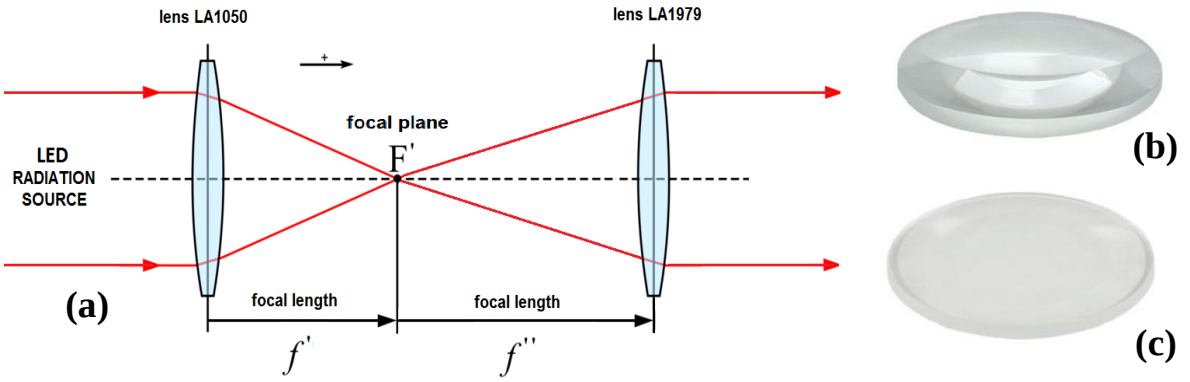

Figure 20. Lenses optical configuration used for the light beam collimation before the optical filtering system (a); lenses LA1050 (b) and LA1979 (c).

V. SYSTEM POWER SUPPLY: CIRCUITAL SOLUTIONS AND USED ICS AND DEVICES

As aforementioned in the introduction, the designed system has a double chance for the power supply, by using the ac main voltage and ac/DC converter or by a battery charged with a properly sized solar panel to achieve a portable system, as reported in figure 21a. The whole spectrophotometer with its different sections (electronic and electro-mechanical) is fed by 12V DC supply voltage that can be provided by means of a DC power supply (shown in figure 21b) powered by the ac main voltage or with a system employing a small solar panel and related battery, as discussed below.

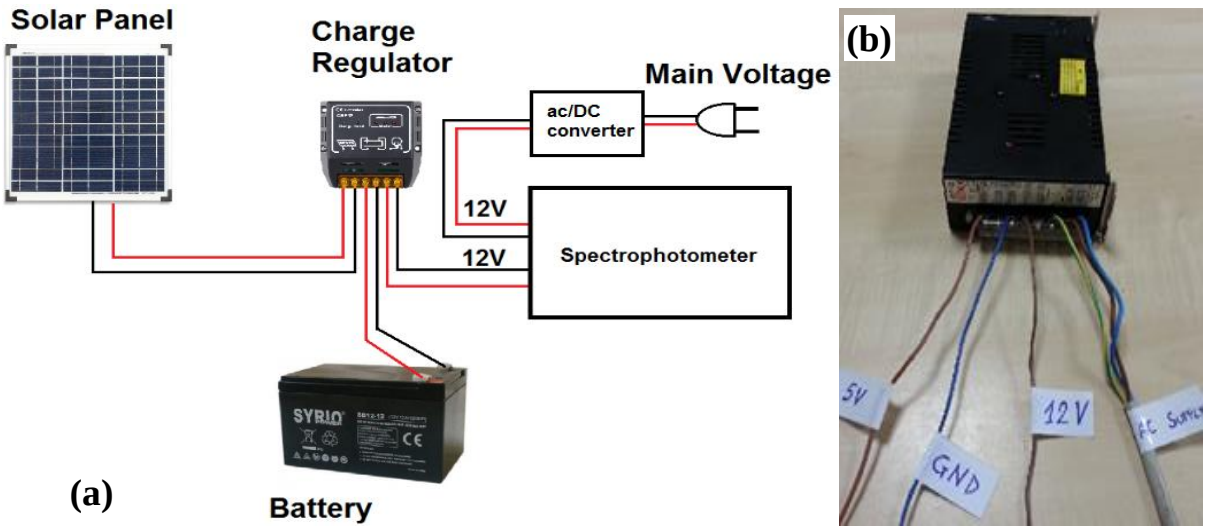

Figure 21. Power supply modes of the spectrophotometer, by solar panel and related battery or through ac main voltage and ac/DC converter (a) and used ac/DC converter (namely a DC Power supply) (b) to feed the whole spectrophotometer.

In the following figure, the power supply circuital scheme related to each sensor and integrated circuit with their respective PIC connection is shown; the system is supplied by DC power supply connected to the main voltage or by the battery charged with the solar panel.

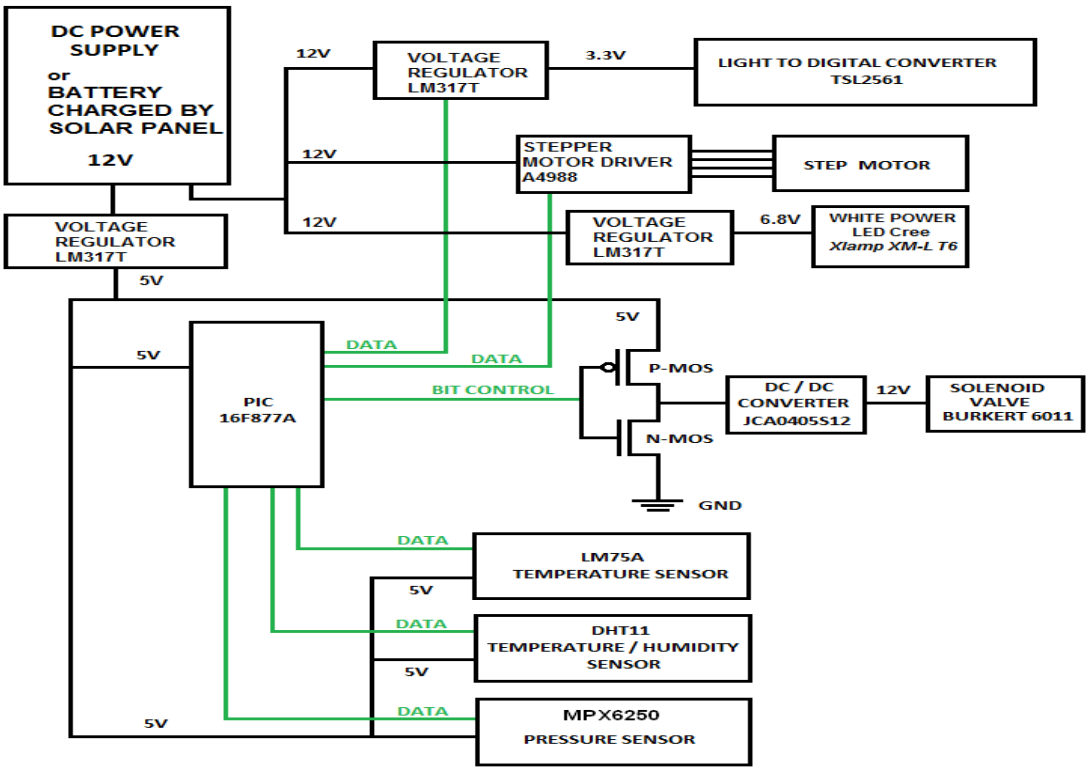

Figure 22. Circuital scheme of the system power supply for providing the proper voltage values required by the various components.

As reported in the previous figure, the luminosity sensor is fed with 3.3V DC voltage provided by the LM317 voltage regulator (shown in figure 23a). It converts the 12V DC input voltage in 3.3V DC output voltage; in particular, it can provide current until 1.5A and withstand a output voltage difference between input and output of 40V. The LM317T device has 3 pin: *input*, *output* and *adjust*. The voltage adjustment occurs by connecting the *adjust* pin to a fixed circuitry (a voltage divider, as reported in figure 23b, is the simplest solution) and keeping a fixed voltage drop of 1.25V (V_{REF}) between output and adjust pin. In this case, the output voltage can be expressed as follow:

$$V_{out} = \left(1 + \frac{R_2}{R_1}\right) * V_{in} + I_{adj} * R_2$$

where R_1 and R_2 are the resistor values, V_{in} the input voltage and I_{adj} the output current from adjust terminal (its maximum value is 100µA as reported in the datasheet).

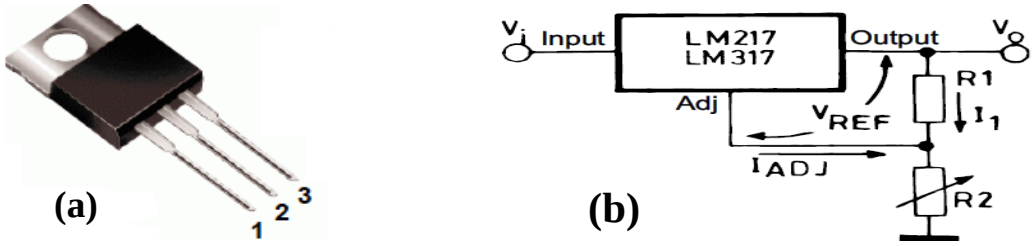

Figure 23. LM317 package screeshot (a) and relative biasing circuit to obtain, in this case, 3.3V used for feeding the luminosity sensor (b).

By using the output voltage expression and fixing the R_1 resistor value to 1kΩ, the R_2 value equal to 1.5kΩ was calculated in order to obtain an output voltage of 3.3V. Furthermore, for PIC power supply, another LM317T voltage regulator, configured as reported in figure 23b, is employed. In this case, the R_1 and R_2 resistor values are 1kΩ and 2,8kΩ respectively thus obtaining the proper supply voltage of 5V. This voltage value, provided by the LM317T, is also used to feed the other sensors present in the system: LM75A temperature sensor (which requires a supply voltage between 2.8 to 5.5V), the pressure sensor MPX6250 (which needs a DC power supply in the range between 4.85V and 5.35V) and the moisture sensor DHT11 that requires a voltage value between 3V and 5.5V. Furthermore, the stepper motor used to actuate the optical filtering system is driven by the stepper motor driver (A4988) which operates from 8 to 35 V. Therefore, to feed the A4988 device, the 12V DC provided by the DC power supply or from the battery were used. In order to properly drive the solenoid valve, with correct voltage and current values, a DC-DC step-up converter, model JCA0405S12, shown in figure 24 was used. It converts the PIC's output voltage level (5V) into the suitable voltage level (12V) for driving the solenoid valve.

Figure 24. View of the JCA0405S12 DC-DC converter, used to step-up to 12V DC the 5V DC provided by the relative microcontroller output pin.

The converter operates with an input DC voltage between 4.5V and 9V and an input current of 975mA (fully loaded). This last current value can't be provided by PIC pin, therefore, to drive the DC-DC conveter, an NMOS and PMOS transistors connected as a CMOS inverter (as shown in figure 22) are used; in this way, PIC provides only the driving signal in negative logic. The two MOS transistors, chosen with an operative current greater than 1A in order to properly drive the DC-DC converter, are reported in figure 25.

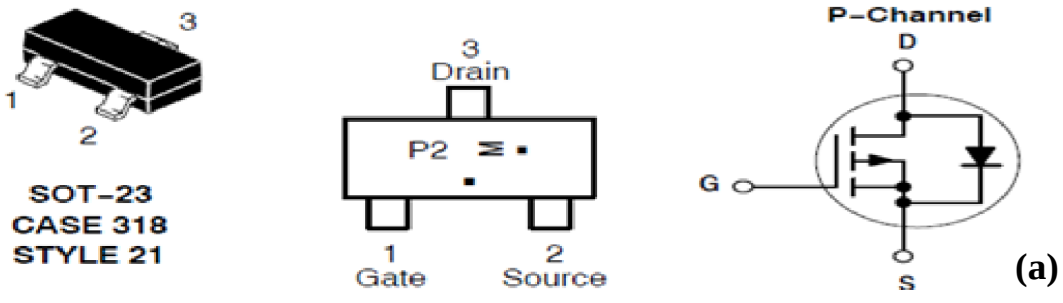

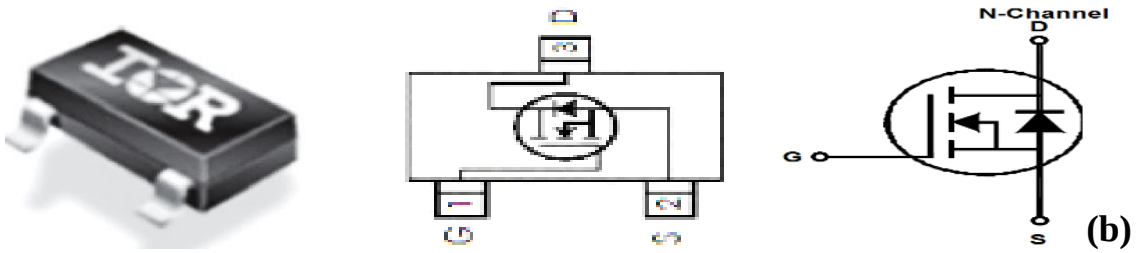

Figure 25. View of package, internal scheme and electrical symbol of the selected PMOS (a) and NMOS (b) used to drive the JCA0405S12 DC-DC step-up converter.

As shown in figure 21a, the 12V power supply used to feed the whole system can be provided also by a 12V 3Ah battery (an example is shown in figure 26c), charged by a PV panel (shown in figure 26a), with nominal power of at least 15W. The battery charging is regulated by the charge regulator *I9Q 5A 12V Charge regulator* shown in figure 26b.

Figure 26. 15W photovoltaic panel used for battery charging to feed system (a), *I9Q 5A 12V* charge regulator (b) and 12V and 3Ah battery (c).

The solar power system has been dimensioned by estimating the spectrophotometer power consumption, taking into account an operative time duration of 2 hours in one day. Considering an operation time of the stepper motor and solenoid valve of only 20% in the 2 hours (in fact, the two devices are not used continuously in the measurement cycle), in order to calculate the system power consumption, the following formulas were used:

*System consumption = LED Power * 2h + Stepper Motor Power * 0.4h + Electronic section Power * 2h + Solenoid Valve Power * 0.4h = 10W * 2h + 6W * 0.4h + 1.5W * 2h + 4W * 0.4h = 27Wh*

Applying a common method to find out the right power value of the PV panel, it means to consider the equivalent lighting hours (in our case, two hours assuming to be in the winter season, as worst case), the minimum solar panel power is obtained as follows:

$$Solar\ panel\ Power = \frac{System\ consumption}{equivalent\ lighting\ hours} = \frac{27Wh}{2h} = 13.5\ W$$

Therefore, a 15W PV panel was chosen to ensure greater autonomy. Regarding the battery, assuming 1 day of system autonomy (with absolute absence of solar energy), the calculated battery capacity is given by the following formula:

$$Battery\ capacity = \frac{System\ consumption * Autonomy\ hours}{Power\ supply\ Voltage} = \frac{27Wh * 1day}{12V} = 2.25Ah$$

Thus, in order to obtain a system with greater power autonomy, a 3Ah battery was chosen (as shown in figure 26c).

VI. FLOWCHART OF THE SYSTEM OPERATION AND RELATED IMPLEMENTED FIRMWARE

The spectrophotometer operation is reported in the simplified flowchart shown in figure 27. Once started the PC-MCU communication, the user can choose to set, by terminal, the measurement parameters (maximum and minimum temperature and reference pressure) or to use the default parameters (ΔT= [20 - 40]°C, P = 200kPa). Subsequently, the user can command, by terminal, the measurement cycle starting; the system acquires chamber pressure, temperature and humidity values and displays them on PC terminal.

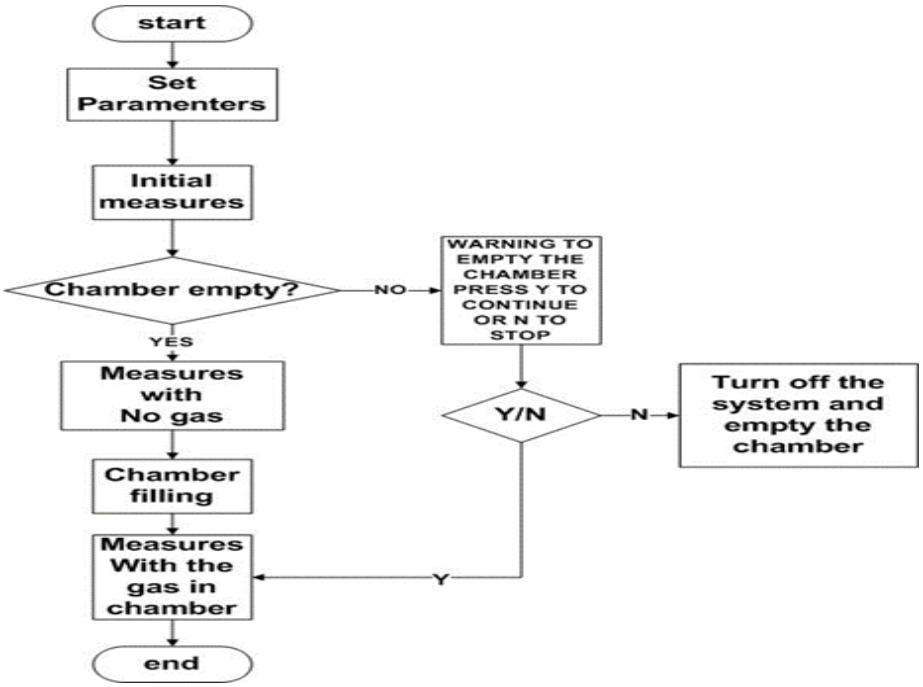

Figure 27. Semplified flow-chart of the developed firmware, with indicated the tasks sequence performed by the system.

If any gas is already present in the chamber, the user can decide to stop or to proceed with the measurement cycle. In this last case, the luminous intensity value, for each wavelength range selected by the proper optical filter, is acquired. Conversely, if the chamber is empty, the

system detects the luminous intensity as function of the wavelength range, varying optical filters, for the next normalization step. Then, to load gas in the chamber, the control unit actuates the solenoid valve, keeping it open until the pressure reaches the reference value; at the end of this phase, a temperature verification is performed. If it's out of the setting range, the system stops the measurement cycle and it displays a warning message on PC terminal. Otherwise, the system proceeds by measuring the luminous intensity of the transmitted radiation, but also by acquiring the pressure and temperature values, for each wavelength range. These values are displayed on PC distinguishing them for each wavelength range. By comparing the values of transmitted radiation intensity acquired for each wavelength range, with and without gas in the chamber, the gas absorption spectrum can be extracted.

A set of functions implemented in the firmware performs the elementary operations, such as sensor readings and motor driving. The functions are called up in the main firmware to achieve the aforementioned behaviour. The figure 28 shows the firmware section related to the *temperature()* function; it's used to read the 11-bit 2's complement data from LM75A *temperature register*. The comunication with the sensor is performed according to the phases determinated by the producer in compliance with the I^2C standard.

```
//Function for temperature measurement (LM75A)

int temperature(){
  unsigned char dato1=0;
  unsigned char dato2=0;
  int valore_conv=0;
  int temperatura=0;

  I2cStart();                    // start sequence
  I2cWriteMaster(0b10010000);    // slave address(000)+ write
  while(ACKSTAT!=0){}            // wait for ACK
  I2cWriteMaster(0b00000000);    // pointer byte to Temp Register
  while(ACKSTAT!=0){}            // wait for ACK
  I2cRepStart();                 // start repeat
  I2cWriteMaster(0b10010001);    // slave address(000)+ read
  while(ACKSTAT!=0){}            // wait for ACK
  dato1=I2cReadMaster(1);        // acquisition of the 8 MSB of detected temp + ACk
  dato2=I2cReadMaster(0);        // acquisition of the 8 LSB of detected temp + NACk
  I2cStop();                     // stop sequence
  valore_conv=((dato1*256)+dato2)/32;// value of the AD conversion
  if((valore_conv&(1<<10))==0){      // Temperature value extraction
   temperatura=valore_conv*0.125;
  }
  else{valore_conv=-1*(((~valore_conv)&0b1111111111)+1);
  temperatura=valore_conv*0.125;
  }
  return temperatura;        // Temperature value
```

Figure 28. Firmware section for I^2C communication between PIC and LM75A sensor with data conversion in the temperature value, highlighted (red line).

Also the luminosity sensor, an essential component for the system operation, uses the I^2C protocol. The data acquisition from light sensor is performed by two functions *read_TSL25Channel0()* and *read_TSL25Channel1()* for reading data from two only *IR* and *IR/VIS* photodiodes; each of these functions accesses to the two 8-bit buffer registers of each

acquisition channel. These two registers, for each channel, contain the most and less significative bytes, related to transmitted light intensity, obtained from 16bit A/D conversion. In particular, the function *read_TSL25Channel0()* is used to read sequentially the data bytes contained in the two buffer registers related to the *Channel0* acquisition channel (with address respectively D_{hex} and C_{hex}), whereas the function *read_TSL25Channel1()* is used to read data bytes relative to *Channel1* acquisition channel (with address respectively F_{hex} and E_{hex}), according to the instruction sequence reported in the paragraph III. Next, the data are processed by another function that converts them in the luminosity value (lux).

Another used digital sensor is the DHT11 temperature-humidity sensor. The communication with PIC occurs via *one wire* protocol. Through a suitable function, MCU can acquire the humidity value according to the phases described in paragraph III; in particular, MCU sends to sensor (slave) the proper logic levels sequence to address it, hence, the sensor responds with its logic levels sequence and sends the 5 bytes data packet, containing the humidity and the temperature data. The implemented function stores only the data relative to the humidity value (integer and decimal part) and displays them on PC-terminal. Finally, the function checks the data packet correctness using the checksum byte.

Another function is implemented to acquire the analog signal level from the pressure sensor, using the analog-to-digital conversion module embedded into the PIC. The firmware implementation of this function is reported in figure 29.

```
//Function to acquire the pressure level from the MPX6250 sensor

unsigned long pressure()
{
    float valore=0;
    int valore_conv=0;
        int pressione=0;

    ADCON0=0b10000001;//set CHS2,CHS1,CHS0 to configure
                      //only AN0 as acquisition channel

    DelayUs(100);
    GO=1;
    while(GO){}
    valore_conv=ADRESL+(ADRESH<<8);
    valore=(valore_conv*4.88);//obtains the signal level expressed in millivolts,
                              //taking account that 1bit=4.88mV
    pressione=(((valore/5000)+0.04)*(1/0.004));
    //invert the sensor transfer function to obtain the pressure value in KPa
    ADIE=0;
    return pressione;
}
```

Figure 29. Firmware section relative to signal level acquisition from the analog pressure sensor MPX6250

In this firmware section, the proper PIC registers to configure the integrated A/D Converter module are set; in particular, the pin AN0 is set as analog input to which the pressure signal is connected and the ADC module performs the conversion process. Then, the function reads the 2 bytes digital pressure data, obtained by the conversion process, from the two buffer registers

(ADRESL and ADRESH). Finally, the function converts the digital data in the pressure value [kPa] by means of the sensor transfer function reported in figure 10d.

Another firmware section is relative to the signals for managing the stepper motor driver (A4988), which actuates the stepper motor used in the optical filtering system. The driver is interfaced with the microcontroller by means of two signals, as indicated in figure 15c, namely *STEP* signal and *DIR* signal. The first is used to control the motor rotation, in particular for each rise front of this signal, the motor rotates by 1.8°, whereas the DIR logic signal specifies the rotation direction ("0" for clockwise and "1" counter-clockwise). In figure 30, the two functions to handle the motor rotation are reported. The function *ruota60_gradi()*, reported in figure 30a, generates a signal to rotate the motor axis by 59.4°; it generates 33 square pulses (to each pulse, a motor rotation of 1.8° corresponds) and also it keeps the DIR signal to "0". Whereas, the function *compensa_err_step()*, reported in figure 30b, is used to generate the signals to compensate the 3.6° angular error accumulated at the end of a complete round of the filter wheel.

```
//Function for rotation of filter wheel
void ruota_60gradi(void){
unsigned char count=0;
MOT_DIR=0;
PWM_DRIVE=0;

for(count=0;count<33;count++)
{PWM_DRIVE=0;
 DelayMs(2);
 PWM_DRIVE=1;
 DelayMs(2);
 }
```

(a)

```
//Function for error compensation
void compensa_err_step(void)
{   unsigned char count=0;
    MOT_DIR=0;
    PWM_DRIVE=0;

    for(count=0;count<2;count++)
    {PWM_DRIVE=0;
     DelayMs(2);
     PWM_DRIVE=1;
     DelayMs(2);
    }
```

(b)

Figure 30. Firmware sections related to the step motor driving: function *ruota60_gradi()* (a) to select the next filter and *compensa_err_step()* (b) to add the appropriate steps for error compensation.

The last firmware section is relative to the main routine, where the previously defined and described functions, used to acquire data from sensors and to synchronize and manage the different system operations, are called up. In particular, the developed firmware section related to the measurement cycle with no gas in the chamber performs reading and processing operations, for each optical filter (wavelength range), of the luminous intensity transmitted through the analyte and then detected by the TSL2561 light sensor. Also, for each iteration of the *for cycle* (corresponding to a different optical filter), PIC sends detected data to PC to display them on terminal and drives motor to rotate the filter holder wheel by 60° for the next iteration. Once completed this phase, system manages chamber filling by opening the solenoid valve until the measured pressure is equal to the reference pressure, as reported in figure 31.

```
//start of the chamber filling(the pressure starts from 0 because it's previously resetted)
    SendByteSerially(0x0D);
    SendByteSerially(0x0D);
    SendStringSerially("FILLING CHAMBER IN PROGRESS");
    SendByteSerially(0x0D);
while(press<press_rif){
    VALVE=0;//open the solenoid valve and enter the gas inthe chamber
    press=pressure();
}
VALVE=1;//close the solenoid valve
SendByteSerially(0x0D);
SendByteSerially(0x0D);
SendStringSerially("FILLING CHAMBER FINISHED");
SendByteSerially(0x0D);
SendByteSerially(0x0D);
DelayMs(100);
temp=temperature();//read the chamber temperature
if((temp<=T_Max) && (temp>=T_min)){
// detect the gas humidity inside the chamber
humidity();
SendByteSerially(0x0D);
```

Figure 31. Firmware section reltive to chamber filling and following conditions check.

Next, after the temperature check, the system performs another measurements cycle with the analyte into the chamber: it's similar to the previous one, but as well as a luminosity measure for each optical filter, it also performs gas temperature and pressure measures. Afterwards, similarly to the previous one, the PIC sends the information to the PC, which displays them on terminal, and drives the motor to rotate the filter holder wheel by 60° for the next iteration.

VII. SOFTWARE SIMULATION OF THE DESIGNED CONTROL UNIT

In order to verify the proper operation of the developed firmware, the control unit was designed using all the components and ICs made available by the used software; afterwards, it was simulated checking the correct operation of the different firmware sections. The designed circuital scheme is reported in figure 32.

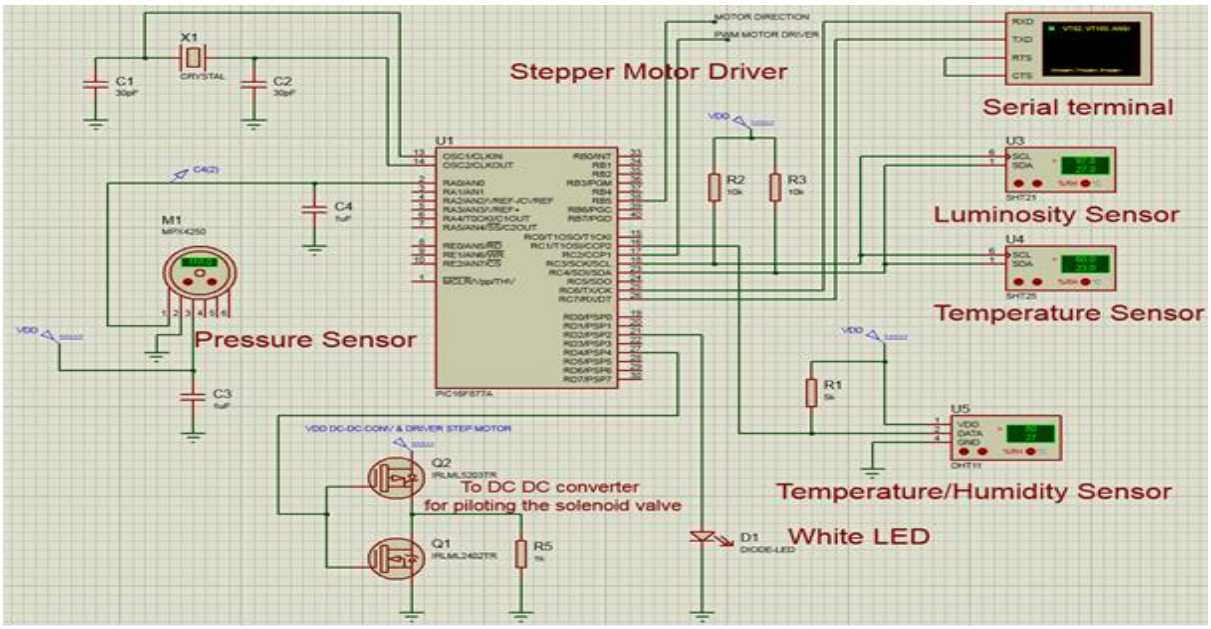

Figure 32. Circuital scheme of the whole control unit, with indicated the different used Integrated Circuits, sensors and components.

Because some sensors chosen and used in the designed control unit were not available in the software library, they were substituted with other sensors with similar features. In particular, the TSL2561 was substituted with the SHT21 humidity-temperature sensor, available in the software library, which presents the same MCU-sensor communication protocol (I^2C) as the TSL2561 luminosity sensor. To verify the correct communication between sensors and PIC, employing I^2C protocol, the *I^2C Debugger*, shown in figure 33, was used. It allows to check the data and the instructions exchanged between the two devices; in fact, considering the row highlighted in red line, the reading from the sensor provides a start signal ("*S*" in figure) followed by the sensor address with a write indication (52_{hex}) sent by PIC that then waits to receive the acknowledgement (ACK) (in this case 52_{hex} isn't the SHT21 sensor address but of the TSL2661 sensor, therefore PIC receives a *NACK* (N) as shown in the I^2C debugger). Next, the master (PIC) sends a command including the desired register address ($8C_{hex}$).

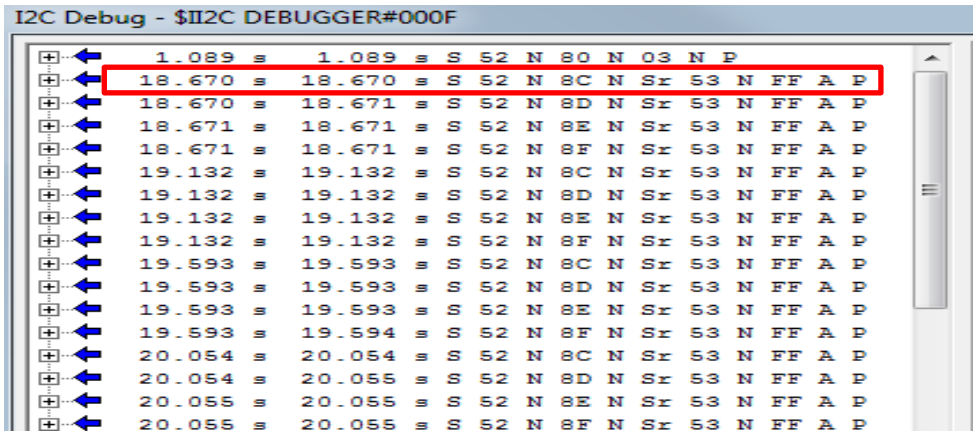

Figure 33. Communication test between PIC and the luminosity sensor (TSL2561) by means of the I^2C debugger.

Now the master can read the acquired data from sensor; after a start repeat command (Sr), the PIC sends again the sensor address but, this time, with a read indication (53_{hex}). At this point, the sensor sends to PIC the acknowledgement (N in this case) followed by the 16-bit data (FF_{hex}); finally, master sends the acknowledgement followed by the stop signal (P). In this way, the firmware section related to the I^2C communication protocol for PIC-TSL2561 data exchange, complying the producer guidelines reported in paragraph III, was checked.

Similarly, the LM75A temperature sensor was not available in the software library, hence, it was substituted by SHT25 temperature sensor that uses the same communication protocol (I^2C); also in this case the I^2C Debugger was used to check correct PIC-sensor communication. For the reading of analog voltage value provided from MPX6250 pressure sensor, the A/D Converter module integrated in PIC16F877A was used; the implemented function is called up in the main firmware section when the sensor reading is required. For the DHT11 temperature

and humidity sensor, it wasn't possible to test the firmware operation in the simulation phase; in fact, the sensor wasn't present in the software libraries and no similar device, with the same communication protocol (*one-wire*), was available in the libraries.

✓ ***Developed firmware testing***

Once launched the simulation, the Virtual Terminal, a window used to simulate the PC-terminal presence, shows the sent data by the MCU to PC, through the serial communication. In figure 34, the virtual terminal screenshot, just after the simulation starting, is shown.

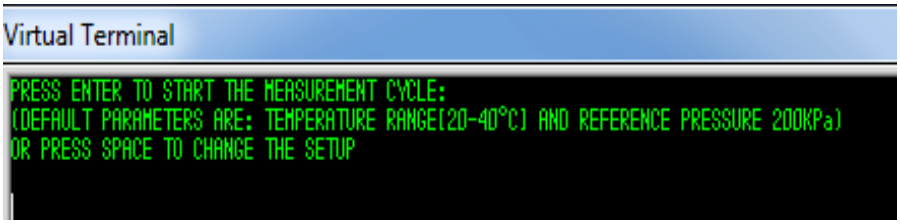

Figure 34. Virtual Terminal (that simulates the presence of PC) by the user can set the measurement parameters and displays data about the measurements cycle in progress.

The user can choose to perform a measurement cycle using the default parameters (defined in the firmware equal to 20÷40°C for the temperature range and to 200kPa for reference pressure) pressing *ENTER*, or to change them by pressing the *SPACE* bar. If the user presses *ENTER*, the terminal displays the message "START MEASUREMENT CYCLE" and the chamber pressure, temperature and humidity values are shown. If the detected pressure is lower or equal than the atmosferic pressure, the control unit performs the luminosity measurement for each selected (by the filtering system) wavelength range. In particular, the system starts with the luminous intensity measurements, indicated as "RADIANCE" on virtual terminal and highlighted in blu in figure 35, with no gas in the chamber for each wavelength range. Then, the control unit handles the chamber filling opening the solenoid valve and displaying on terminal the warning "FILLING CHAMBER IN PROGRESS"; this phase finishes when chamber pressure is equal to the reference pressure, the solenoid valve is closed and the message "CHAMBER FILLING FINISHED" is shown on terminal. Now, the control unit newly performs an humidity reading displaying the measured value on virtual terminal. Subsequently, the system performs a measurement cycle with the gas inside the chamber, phase highlighted in red in figure 35. It displays the luminous intensity values acquired by the TSL2561 luminosity sensor (indicated as RADIANCE in figure 35), the temperature value detected by SHT25 sensor (indicated as TEMPERATURE in figure 35) and the gas pressure value measured by the MPX6250 analog pressure sensor, (indicated as PRESSURE in figure 35). All these values are displayed for each

wavelength range (as a function of the optical filter selected on the optical filtering system). Finally the system prompts the user to press ENTER to restart the measurements cycle.

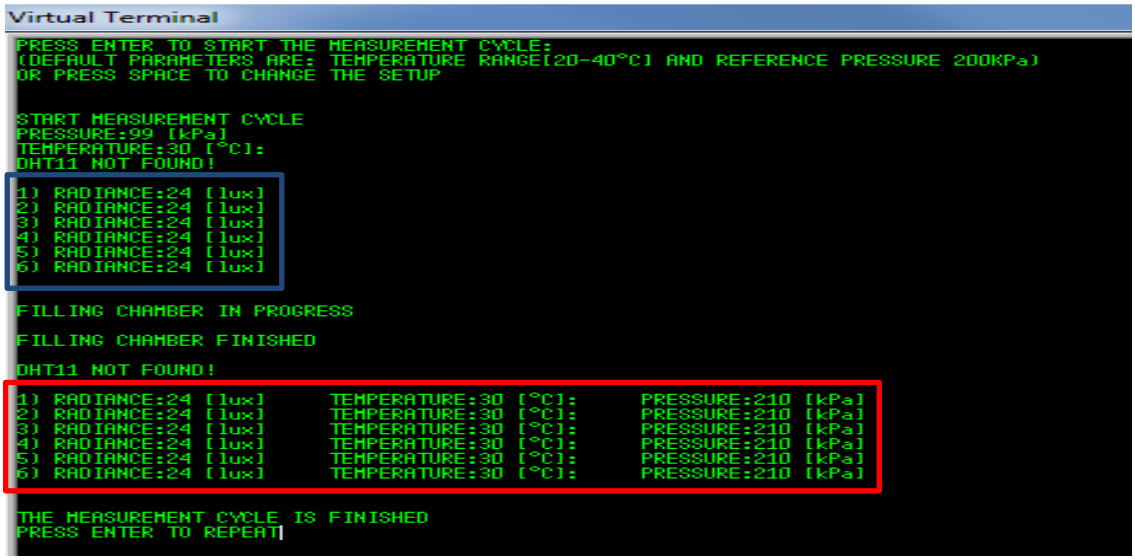

Figure 35. Virtual Terminal screenshot during the whole measurement cycle.

If any gas is already present in the chamber, before starting a new measurement cycle, the control unit prompts the user to choose if to continue the measurement cycle, pressing “Y”, or stopping it and to empty the chamber by pressing “N”. In the first case, the control unit performs the normal measurement cycle without emptying the chamber; in this case, the gas temperature and pressure values, besides the luminous intensity of light beam after passing through the gas, are detected for each wavelenght range (optical filter), as previously described. Once completed the measurement cycle, the system prompts the user to press *ENTER* to restart the measurement cycle. Otherwise, in the second case, the terminal displays the warning message inviting the user to empty the chamber.

VIII. COMPLETE SYSTEM ASSEMBLING AND CONCLUSIONS

The different electronic and mechanical sections of the realized spectrophtometer were put together, as shown in figure 36a. The setup is composed of the electronic control board, the optical filtering system, the white LED radiation source, PC and the measurement chamber with the proper wiring of different sensors (humidity, temperature and pressure) positioned inside the chamber and the luminosity sensor outside in front of the plexiglass wall. The white LED radiation source is placed in front to the passing hole present on the aluminium structure of the optical filtering system (as shown in figure 36b). Then, after the wavelength range selection by means of the optical selective filters, the filtered light beam enters in the

measurement chamber interacting with gas if present. The measurement chamber consists of a plexiglass cylinder, covered with a black sheath, with diameter equal to 10cm, sealed at the ends by two transparent plexiglass walls. The different chamber parts (the two walls with the cylinder) are held together by 8 threaded rods as shown in the figures 36b and 36c; on the chamber frontal wall, two valves are placed for grafting of the two ducts for gas inlet and outlet (figure 36c). In figure 36d, the TSL2561 luminosity sensor positioned on the realized support, in front of the transmitted radiation beam, is shown.

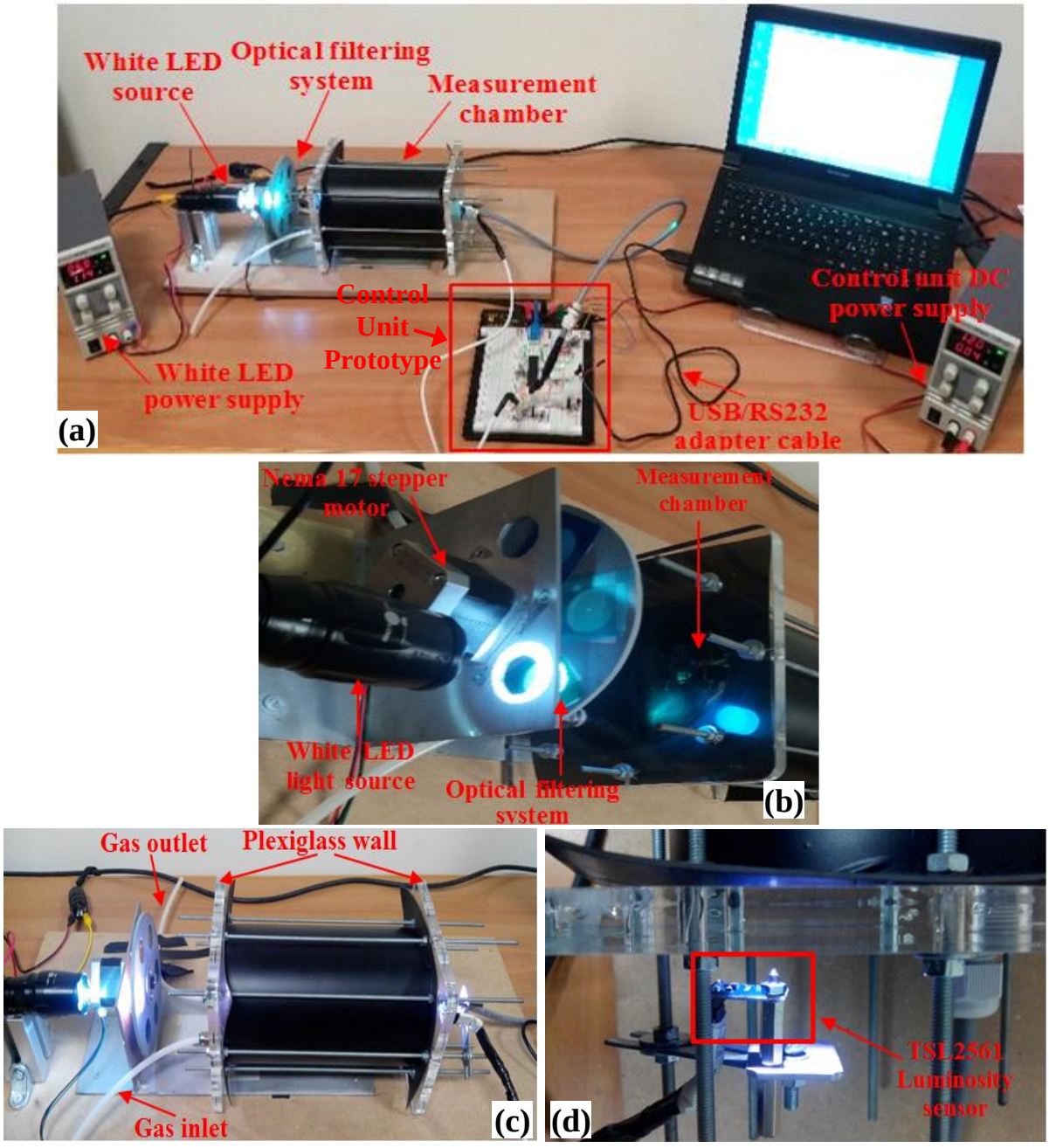

Figure 36. View of the whole spectrophotometer prototype with highlighted the different sections (a), light radiation passing through the aluminium structure hole (b), view of the spectrophotometer with the white LED radiation source, optical filtering system and the measurement chamber (c) and luminosity sensor highlighted placed in front of chamber wall.

Finally, the full spectrophotometer's operation was checked to verify the proper execution and scheduling of the different firmware sections; by viewing on PC terminal the data and informations sent from the control unit to PC, it is possible to monitor and follow the system operation. In fact, the control unit sends, through the USB-RS232 adapter cable, the measures acquired during the measurement cycle and the information relative to the system status (i.e. waiting for parameters insertion by the user, chamber status whether full or empty, measurement cycle in progress). In addition, the system-user interaction, by sending starting or stopping commands or by setting parameters, was verified. Therefore, a full verification of the realized system operation was performed analyzing the proper execution of the different functionalities: the sensors-PIC data exchange, control unit-PC communication, the actuating of the stepper motor and of the solenoid valve thus confirming the correct system operation and interaction with the user.

REFERENCES

[1]. Q. Li, F. Wang, Z. Aleck Wang, D. Yuan, M. Dai, J. Chen, J. Dai, K. A. Hoering: Automated Spectrophotometric Analyzer for Rapid Single-Point Titration of Seawater Total Alkalinity. Environmental Science & Technology - ACS, Vol 47, pp. 11139 – 11146, (2013).

[2]. A. Lay-Ekuakille, P. Vergallo, R. Morello, C. De Capua: Indoor air pollution system based on LED technology. Measurement, Vol. 47, pp. 749 – 755, (2013).

[3]. A. Lay-Ekuakille, I. Palamara, D. Caratelli, F. C. Morabito: Experimental infrared measurements for hydrocarbon pollutant determination in subterranean waters. Review of Scientific Instruments, Vol. 85, pp. 015103-1 - 015103-8, (2013).

[4]. A. Lay-Ekuakille, G. Vendramin, A. Trotta: LED-based sensing system for biomedical gas monitoring: Design and experimentation of a photoacoustic chamber, Sensors and Actuators B, Vol. 135, pp. 411–419, (2008).

[5]. K. Laqua, W.H. Melhuish, M. Zander: Molecular Absorption Spectroscopy, Ultraviolet and Visible (UV/VIS). Pure & Applied Chemistry, Vol. 60, No. 9, pp. 1449 – 1460, (1988).

[6]. P. Visconti, A. Lay-Ekuakille, P. Primiceri, G. Cavalera: Wireless Energy Monitoring System of Photovoltaic Plants with Smart Anti-Theft Solution Integrated with Control Unit of Household Electrical Consumption. International Journal on Smart Sensing and Intelligent Systems, Vol. 9, No. 2, pp. 681 – 708, (2016).

[7]. P. Visconti, R. Ferri, M. Pucciarelli, E. Venere: Development and Characterization of a solar-based energy harvesting and power management system for a WSN node applied to optimized goods transport and storage. International Journal on Smart Sensing and Intelligent Systems, Vol. 9 (Issue 4), pp. 1637 – 1667, (2016).

[8]. M. Lepot, A. Torres, T. Hofer, N. Caradot, G. Gruber, J.-B. Aubin, J.-L. Bertrand-Krajewski: Calibration of UV/Vis spectrophotometers: A review and comparison of different methods to estimate TSS and total and dissolved COD concentrations in sewers, WWTPs and rivers. Water Research, Vol. 101, pp. 519-534, (2016).

[9]. P. Primiceri, P. Visconti, A. Melpignano, A. Vilei. G. M. Colleoni: Hardware and software solution developed in ARM mbed environment for driving and controlling DC brushless motors based on ST X-NUCLEO development boards. International Journal on Smart Sensing and Intelligent Systems, Vol. 9, No. 3, pp.1534–1562, (2016).

[10]. E. Lunca, S. Ursache, A. Vasniuc: Temperature Monitoring System Based on Multiple TMP75 Digital Sensors and the PC's Parallel Port. Proc. of 9th Int. Symposium On Advanced Topics In Electrical Engineering, DOI:10.1109/ATEE.2015.7133668, (2015).

[11]. P. Visconti, C. Orlando, P. Primiceri: Solar Powered WSN for monitoring environment and soil parameters by specific app for mobile devices usable for early flood prediction or water savings. Proceeding of IEEE 16th Int. Conference on Environment and Electrical Engineering – EEEIC 2016, DOI:10.1109/EEEIC.2016.7555638, pp.1–6, (2016).

[12]. M. Jankovec, F. Galliano, E. Annigoni, H. Yu Li, F. Sculati-Meillaud, L.E. Perret-Aebi, C. Ballif, M. Topič: In-Situ Monitoring of Moisture Ingress in PV Modules Using Digital Humidity Sensor. IEEE Journal of Photovoltaics, Vol.6, pp.1152-1159, (2016).

[13]. P. Visconti, P. Primiceri, G. Cavalera: Wireless monitoring and driving system of household facilities for power consumption savings remotely controlled by Internet. IEEE Proceeding of 2016 Workshop on Environmental, Energy and Structural Monitoring Systems, (EESMS), DOI: 10.1109/EESMS.2016.7504805, pp. 1 – 6, (2016).

[14]. P. Visconti, P. Primiceri, P. Costantini, G. Colangelo, G. Cavalera: Measurement and control system for thermo-solar plant and performance comparison between traditional and nanofluid solar thermal collectors. International Journal on Smart Sensing and Intelligent Systems, Vol. 9 (Issue 3), pp. 1220 – 1242, (2016).

[15]. S. Sinha, D. Banerjee, N. Mandal, R. Sarkar, S. C. Bera: Design and Implementation of Real-Time Flow Measurement System Using Hall Probe Sensor and PC-Based SCADA. IEEE Sensors Journal, Vol. 15, No. 10, pp. 5592 – 5600, (2015).